A New Approach to Enhance the Torque Handling Capacity of a PMBLDC Motor Drive

Protik Chandra Biswas[*], Bashudeb Chandra Ghosh

Department of Electrical and Electronic Engineering, Khulna University of Engineering & Technology, Khulna, Bangladesh
*Corresponding author: protikpc07@gmail.com

Abstract Permanent Magnet Brushless DC (PMBLDC) Motors are trapezoidal shaped back EMF permanent magnet AC machine with high power density. Since the motor has a trapezoidal field pattern rather than sinusoidal it is desirable to study the motor behavior under different current fed conditions to analyze the developed electromagnetic torque. In this paper three different trapezoidal, square and sinusoidal current fed field oriented vector controlled PMBLDC motor drives are presented. The novel approach of this paper is that, the torque handling capacity of a PMBLDC motor can be increased up to its rated torque by only changing the pattern of reference current of a field oriented vector controlled PMBLDC motor drive. Adaptive PI controller based on motor speed error is also proposed in the paper to have a simplified drive system. When square and sinusoidal reference current fed vector controlled drives are used, the maximum torque handling capacity of a specified PMBLDC motor is 1.60 Nm and 1.55 Nm respectively. Only by using trapezoidal reference current fed drive, the maximum torque handling capacity of that specified motor can be increased to 2.0 Nm. The performance of these three different current drives are also compared on the basis of their torque pulsation. The dynamic performance of the vector controlled trapezoidal current fed drive is found outstanding than the square and sinusoidal current fed drives considering response time, load torque handling capacity, variable speed condition, settling time of the system.

Keywords: *Field Oriented Control, Permanent Magnet Brushless DC (PMBLDC) motor drives, Trapezoidal Current Fed System, Adaptive PI Controller*

Cite This Article: Protik Chandra Biswas, and Bashudeb Chandra Ghosh, "A New Approach to Enhance the Torque Handling Capacity of a PMBLDC Motor Drive." *American Journal of Electrical and Electronic Engineering*, vol. 4, no. 6 (2016): 164-176. doi: 10.12691/ajeee-4-6-3.

1. Introduction

Now a days converter fed machines (CFMs) become more popular. A typical example of CFMs is the Permanent Magnet Brushless DC (PMBLDC) motor [1]. Permanent Magnet Brushless DC (PMBLDC) motors are extensively used as an industrial motor due to their fast dynamic response, high power density, large torque to inertia ratio, higher efficiency with increased reliability, less noise, longer life, silent operation, compact form, low maintenance and better controllability [2,3]. For innumerous applications, PMBLDC motors are used as a replacement for AC motors and these motors also reduce the overall system weight. The commutation of BLDC motor is done electronically, hence it is quite simple to control the torque and RPM of the motor even at much higher speed [4].

Permanent Magnet AC (PMAC) and Permanent Magnet DC (PMDC) machines are two types of permanent magnet electric machines. Depending on the type of back EMF, PMAC machines can be classified into two types. The first type of motor is referred to as Permanent Magnet Synchronous Motors (PMSM). These produce sinusoidal back EMF and should be supplied with sinusoidal current. The second type of PMAC motor is called Permanent

Magnet Brushless DC (PMBLDC) motors because of its trapezoidal shaped back EMF and rectangular shaped currents are to be fed to these motors [5]. The PMDC machines are similar with the DC commutator machines, the only difference is that permanent magnets are used instead of the electromagnetic field windings. Besides in case of PMBLDC motor, the field is generated by the permanent magnets placed on the rotor, the brushes and the commutator does not exist in this machine type. For this reason the PMBLDC motor is simpler and more attractive to use instead of PMDC [6].

The transformation of machine equations to the well-known d, q reference frame is not appropriate for modeling and simulation of PMBLDC motor drives because of the trapezoidal back EMF and the consequent no sinusoidal variation of the motor inductances with rotor angle. For non-sinusoidal flux distribution, it is prudent to drive a model of the PMBLDC motor in natural or phase variables [6,7].

Generally current control is used in PMBLDC drives by assuming that torque is proportional to the phase current. In practice to minimize torque pulsation, various current control strategies are used. An optimal current excitation scheme which resulted ripple-free torque is proposed in [8]. A simple predicted current control scheme for PMBLDC motor to reduce the torque ripple in the commutation and conduction region is used in [9] to keep

the constant torque during the conduction and commutation region. In this proposed control system, the inverse function of back EMF is used to consider the back EMF characteristic in the conduction region. Field oriented control of a PMBLDC motor to produce a significantly reduced torque ripple is proposed in [10]. A standard mathematical model of a BLDC motor in the a, b, c reference frame which is suitable for simulation of the six-step control strategy, and a mathematical model of a BLDC motor in the d, q reference frame suitable for standard and modified field oriented control strategies are presented through this paper.

In a conventional commutation method current amplitude is kept constant, but in [11] current amplitude is adapted to the rotor position to reduce the torque ripple in PMBLDC motor drives. For this purpose, an optimum reference current is computed based on the phase back-EMF waveform. Comparison of the PWM control and the PAM control for high-speed PMBLDC motor is introduced in [12]. PMBLDC motor can be driven by either Pulse-Width Modulation (PWM) techniques with a constant DC-link voltage or Pulse-Amplitude Modulation (PAM) techniques with an adjustable DC-link voltage. This paper messaged that for high speed operation PAM control is superior to the PWM control. In our paper PWM technique is used. Extreme high speed condition is not considered because it is out of scope of this paper.

In this paper, field oriented control of a PMBLDC motor with three different current fed drives are presented. This paper shows how the torque handling capacity of a PMBLDC motor can be increased up to its rated torque by only changing the reference current of PWM modulator. One of important issue of this paper is that, toque handling capacity is enhanced without exceeds the maximum current rating of the PMBLDC motor. Conventionly square and sinusoidal current fed PMBLDC motor drives are implemented [5,12]. In this paper novel trapezoidal current fed drive is proposed because of the trapezoidal shaped back EMF of PMBLDC motor. The scenario of torque pulsation is also depicted individually for these three different current drives. A hysteresis type current controller is proposed and implemented to maintain the actual current flowing into the motor as close as possible to the reference current. The drive system is simulated in a C++ environment in discrete form. Transient response, loading capability of the motor and dynamic system performance of PMBLDC motor are studied for these three different current fed drives.

2. Mathematical Model of PMBLDC Motor

The flux distribution in BLDC motor is trapezoidal and therefore the d-q axes rotor reference frame model is not applicable. For this non-sinusoidal flux distribution, it is suitable to drive a model of PMBLDC motor on the basis of phase variables. The permanent magnet creates trapezoidal field. Therefore the back EMF's are also trapezoidal as given in Eq. (1).

$$\begin{bmatrix} e_a \\ e_b \\ e_c \end{bmatrix} = \omega_m \lambda_m \begin{bmatrix} f_{as}(\theta_r) \\ f_{bs}(\theta_r) \\ f_{cs}(\theta_r) \end{bmatrix} \tag{1}$$

Where, λ_m is the flux linkage, ω_m is angular rotor speed in radian per second, θ_r is the rotor position in radian and $f_{as}(\theta_r), f_{bs}(\theta_r)$ and $f_{cs}(\theta_r)$ are the flux function of rotor position having the same of 3-phase back EMF with a maximum value of ± 1. Only the flux function $f_{as}(\theta_r)$ is described in Eq. (2). The $f_{bs}(\theta_r), f_{cs}(\theta_r)$ are similar to $f_{as}(\theta_r)$ but 120° phase displacement have to be considered.

$$f_{as}(\theta_r) = \begin{cases} \theta_r \dfrac{6}{\pi}, & 0 \le \theta_r < \dfrac{\pi}{6} \\ 1, & \dfrac{\pi}{6} \le \theta_r < \dfrac{5\pi}{6} \\ (\pi - \theta_r)\dfrac{6}{\pi}, & \dfrac{5\pi}{6} \le \theta_r < \dfrac{7\pi}{6} \\ -1, & \dfrac{7\pi}{6} \le \theta_r < \dfrac{11\pi}{6} \\ (\theta_r - 2\pi)\dfrac{6}{\pi}, & \dfrac{11\pi}{6} \le \theta_r < 2\pi \end{cases} \tag{2}$$

Classical modeling equations are used to model the PMBLDC motor and hence the motor model is highly flexible. These equations are based on the dynamic equivalent circuit of PMBLDC motor. Resistance of all the phase windings are assumed to be equal to R_s. By considering ideal non-salient rotor with uniform reluctance reduces the three phase voltage equation to the form as shown in Eq. 3.

$$\begin{bmatrix} V_{as} \\ V_{bs} \\ V_{cs} \end{bmatrix} = \begin{bmatrix} R_s & 0 & 0 \\ 0 & R_s & 0 \\ 0 & 0 & R_s \end{bmatrix} \begin{bmatrix} i_a \\ i_b \\ i_c \end{bmatrix} + \dfrac{d}{dt} \begin{bmatrix} L & M & M \\ M & L & M \\ M & M & L \end{bmatrix} \begin{bmatrix} i_a \\ i_b \\ i_c \end{bmatrix} + \begin{bmatrix} e_a \\ e_b \\ e_c \end{bmatrix} \tag{3}$$

Where, V_{as}, V_{bs}, V_{cs} are the phase voltages of stator winding, i_a, i_b, i_c are the stator phase currents, R_s is the stator resistance per phase, $L_{aa} = L_{bb} = L_{cc} = L$ are self-inductance of phase a, b, c respectively, $L_{ab} = L_{bc} = L_{ac} = M$ are mutual inductance between phases. The phase currents of stator are considered to be balanced for no neutral connection

$$i_a + i_b + i_c = 0 \tag{4}$$

$$Mi_b + Mi_c = -Mi_a. \tag{5}$$

Then Eq. (5) is used to simplify inductances matrix. Therefore equations in state space form is

$$\dot{x} = Ax + Bu + Ce \tag{6}$$

Where,

$$x = [i_a \ i_b \ i_c]^t \tag{7}$$

$$u = [V_{as} \ V_{bs} \ V_{cs}]^t \tag{8}$$

$$e = [e_a \ e_b \ e_c]^t \tag{9}$$

$$A = \begin{bmatrix} -\dfrac{R_s}{L-M} & 0 & 0 \\ 0 & -\dfrac{R_s}{L-M} & 0 \\ 0 & 0 & -\dfrac{R_s}{L-M} \end{bmatrix} \tag{10}$$

$$B = \begin{bmatrix} \dfrac{1}{L-M} & 0 & 0 \\ 0 & \dfrac{1}{L-M} & 0 \\ 0 & 0 & \dfrac{1}{L-M} \end{bmatrix} \tag{11}$$

$$C = \begin{bmatrix} -\dfrac{1}{L-M} & 0 & 0 \\ 0 & -\dfrac{1}{L-M} & 0 \\ 0 & 0 & -\dfrac{1}{L-M} \end{bmatrix}. \tag{12}$$

The system consists of two other mechanical variables as described now. The electromagnetic torque developed is given by Eq. (13).

$$T_e = [e_a i_a + e_b i_b + e_c i_c]/\omega_m \ (Nm). \tag{13}$$

If the system moment of inertia J, friction coefficient B is constant and load torque is T_l, then the system motion equation is

$$J\frac{d\omega_m}{dt} + B\omega_m = (T_e - T_l) \tag{14}$$

Where, $J = J_m + J_l$. J_m and J_l are the moment of inertia of motor and load respectively. Electrical rotor speed and position is related by Eq. (15). Here, P is number of poles. The rotor position θ_r repeats every 2π radians

$$\frac{d\theta_r}{dt} = \frac{P}{2}\omega_m. \tag{15}$$

3. Approach to Enhance Torque Handling Capacity

Generally per phase torque is proportional to the product of per phase back EMF and corresponding per phase current. From Figure 1, it is seen that, for square current fed drive of phase 'a', for rotor position 0^0-30^0, the developed electromagnetic torque in phase 'a' is zero because phase current i_{as} at that time is zero. So the distributed flux at that time (0^0-30^0) is unutilized for torque production. At that time same positive electromagnetic torque are developed in phase 'b' and in phase 'c' considering balanced phase system. For rotor position 30^0-60^0, the developed electromagnetic torque in phase 'c' is zero and there are same positive developed torque in phase 'a' and in phase 'b'. Similarly for the shaded region in Figure 1, the motor cannot developed any torque. Theoretically this 120^0 switch on mode is used to generate constant instantaneous total torque by considering the toque developed in each phase.
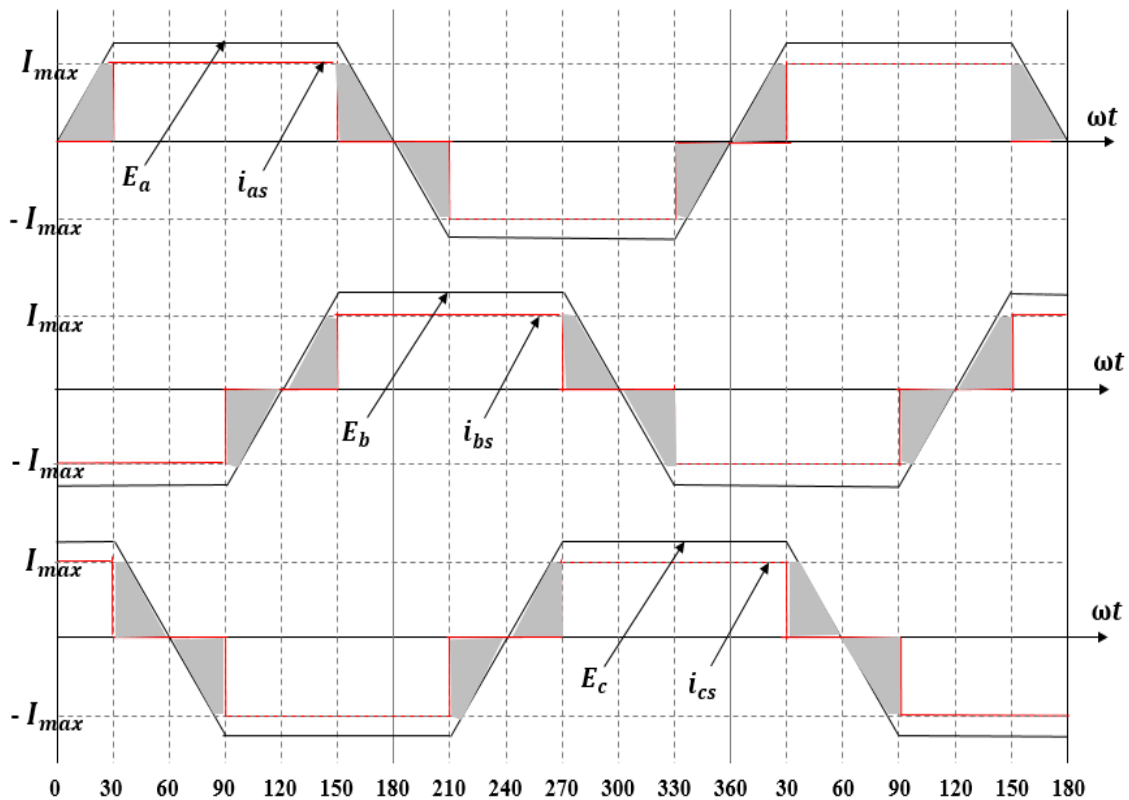
Figure 1. Typical trapezoidal back EMF and square current waveforms of 3-phase PMBLDC motor

Now considering trapezoidal back EMF and trapezoidal reference current waveforms of 3-phase trapezoidal current fed drives as shown in Figure 3. For rotor position 0^0-30^0, there is a positive developed electromagnetic torque in phase 'a' because phase current i_{as} at that time is not zero. Similar to the square wave current fed drive, at that time same positive electromagnetic torque are developed in phase 'b' and in phase 'c'. So additional torque is found from phase 'a' which contributes to the total developed toque at the rotor position 0^0-30^0 for trapezoidal current fed drives. But this additional torque is not generated for square current fed drive. So trapezoidal current fed drive can utilize the flux of that portion of shaded region in Figure 1. Thus torque handling capacity for trapezoidal current fed drive is greater than the square current fed drive. From Figure 3, it is seen that for 0^0-30^0, instantaneous total developed torque is gradually increasing from 0^0 to 30^0, but from 30^0 to 60^0 instantaneous total developed torque is decreasing at the same rate of increasing from 0^0 to 30^0. This scenario is same for other rotor position spans in Figure 3. So for trapezoidal current fed drive the instantaneous total developed toque is not constant, but the average torque is constant.
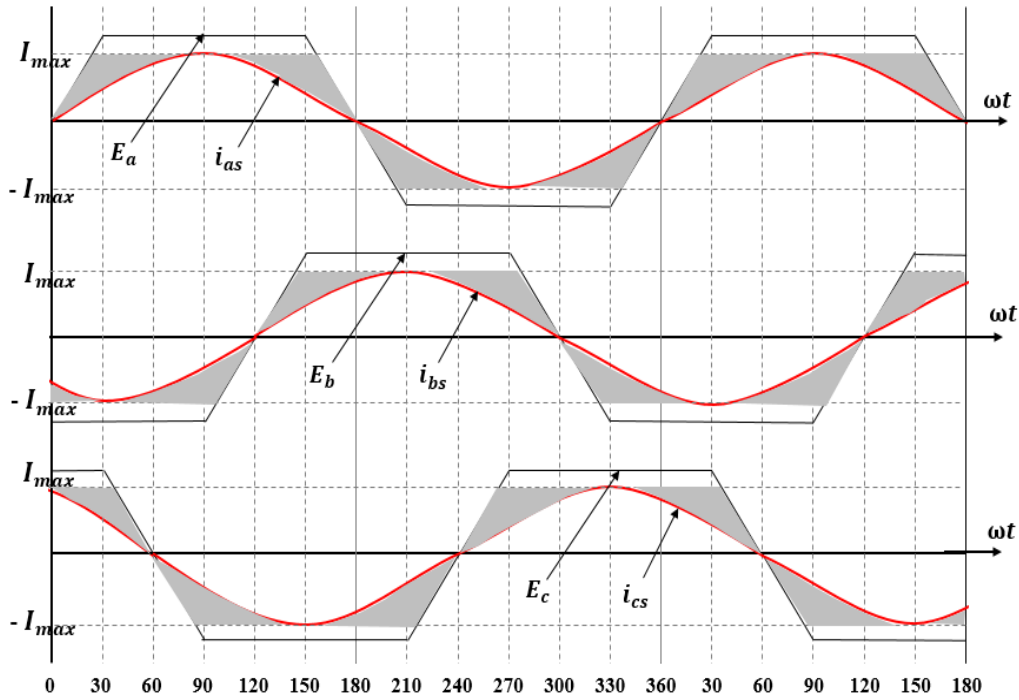
Figure 2. Typical trapezoidal back EMF and sinusoidal current waveforms of 3-phase PMBLDC motor
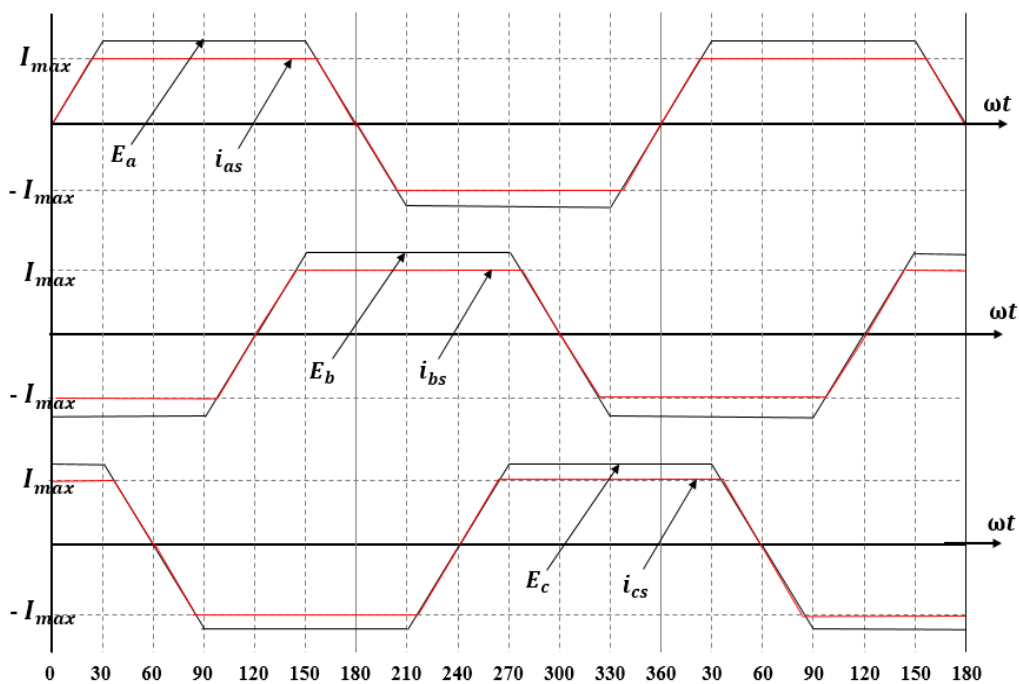
Figure 3. Typical trapezoidal back EMF and trapezoidal current waveforms of 3-phase PMBLDC motor

From the inspection of Figure 2, it can be understood that, the shaded area i.e. the amount of unutilized flux of sinusoidal current fed drive for toque generation is little bit greater than the amount of unutilized flux of square current fed drive. That is the toque handling capacity of sinusoidal current fed drive is less than the toque handling capacity of square current fed drive. So trapezoidal current fed drive is superior on the respect of torque generation. Besides toque handling capacity is increased without exceeds the maximum current rating of the PMBLDC motor. From Figure 1 – Figure 3, it is seen that, for three different current system the maximum value of current is maintained constant value I_{max}. A current limiter is used with adaptive PI speed controller for the purpose to limit the current to the rated value.

4. Proposed Control Scheme

The proposed control drive mainly consists of an adaptive PI controller, field oriented reference current generator, delta modulated PWM current controller, IGBT voltage source inverter, position sensor, current sensors and PMBLDC motor as shown in block diagram in Figure 4. Field oriented controlled three different trapezoidal, square and sinusoidal reference current fed drives for PMBLDC motor control is proposed in this paper to see the scenario of torque handling capacity of these three different reference current drives. The performance of vector controlled trapezoidal current fed drive is compared with traditional square current and sinusoidal current fed vector controlled drive.

4.1. Adaptive PI Controller Design

In a system PI controller attempts to correct the error between actual system variable and desired set point. PI controller is implemented as

$$e_o(t) = K_P e_i(t) + K_I \int_0^t e_i(\tau) d\tau \qquad (16)$$

Where, $e_i(t)$=Desired reference value – Actual value, K_P and K_I are the proportional and integral gains of the PI controller respectively. The actual speed of the PMBLDC motor is compared with its reference speed and the speed error is processed through PI controller to estimate reference toque by Eq. (18).

Speed error,

$$e(t) = \omega_{ref}(t) - \omega_m(t) \qquad (17)$$

$$T_{ref}(t) = T_{ref}(t-1) + K_P \left[e(t) - e(t-1) \right] + K_I e(t). \quad (18)$$

From simulation studies it has been observed that the speed error reduces the effectiveness of the PI controller & becomes slower due to the nonadjustable nature of gain constants. In this control systems K_P and K_I gain constants are made adjustable with speed by using Eq. (19-20). Where, K_{P0} and K_{I0} are initial gain constants of the system, K_1 and K_2 are the constant of the tuner of the proportional and integral gain constants with speed respectively. Ziegler and Nichols second method is used for determining values of the gain constants based on the transient response characteristics of proposed control system. Here $K_{P0} = 2.0$, $K_{I0} = 0.01$, $K_1 = 0.6$ and $K_2 = 0.001$ are selected for these three PMBLDC motor drives. Thus an adaptive PI controller is designed. So that speed overshoot and undershoot in system have to be prevented and settling time to gain reference speed can be minimized.

$$K_P = K_{P0} + K_1 * \omega_m \qquad (19)$$

$$K_I = K_{I0} + K_2 * \omega_m. \qquad (20)$$
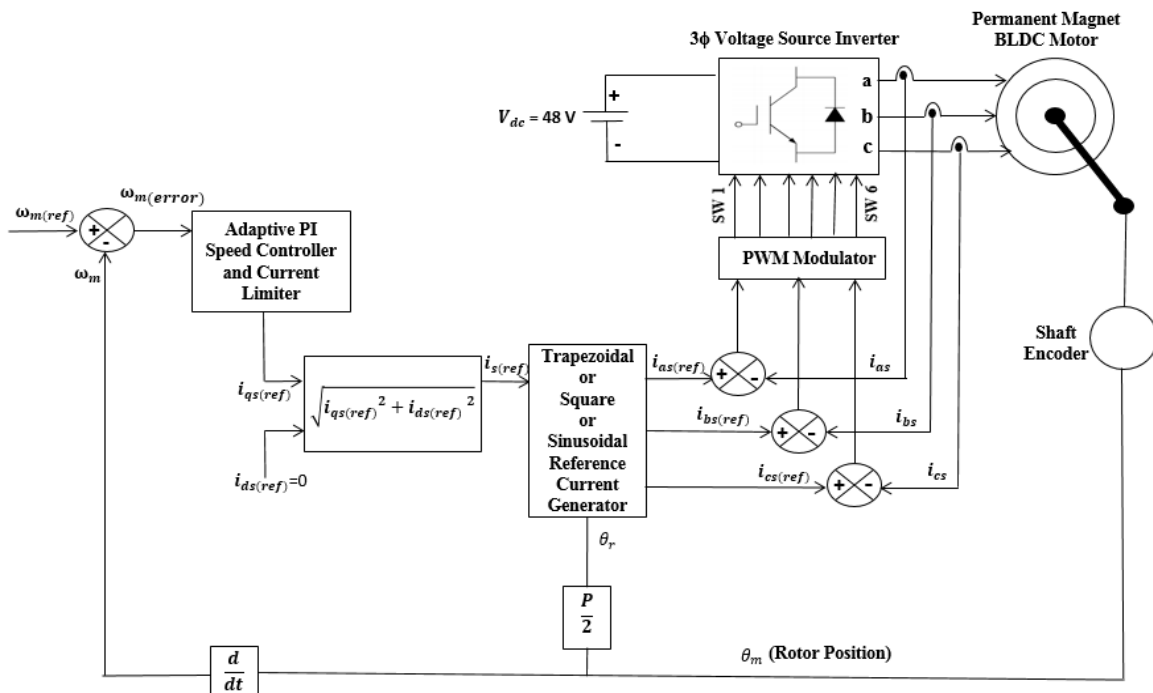
Figure 4. Overall block diagram of trapezoidal or square or sinusoidal current fed field oriented vector controlled PMBLDC motor drives by using adaptive PI speed controller

The output of this adaptive PI speed controller is the reference torque of the system. A limit have to be put on the speed controller output depending on the permissible maximum winding currents. The reference quadrature axis current $i_{qs(ref)}$ is determined from the value of reference torque T_{ref} by using Eq. (21). Where K_t is the torque constant of the PMBLDC motor.

$$i_{qs(ref)} = T_{ref} / K_t. \qquad (21)$$

4.2. Field Oriented Control of PMBLDC Motor Drive

In field oriented control, the direct and quadrature axis current i_d and i_q are controlled to achieve the requested torque. It is possible to achieve a maximum torque per ampere ratio to minimize the current needed for a specific torque by controlling i_d and i_q independently which maximizes the motors efficiency [13]. Direct axis current has no effect on torque production and it needs to be zero at all times to reach maximum torque per ampere ratio. The torque curves will be linear in the d-q plane and the maximum torque per ampere ratio trajectory will be along the quadrature-axis. Field oriented control (FOC) is mainly a mathematical technique utilized for achieving a separate control of the field producing and the torque producing portions of the stator currents in a three-phase motor. Stator current is decomposed into magnetizing current i_d responsible for producing a magnetic field and quadrature current i_q which controls developed torque [14].

In this proposed control system, maximum value of reference current $i_{s(ref)}$ is generated by considering direct axis current $i_{ds(ref)} = 0$ and by calculated the value of quadrature axis current $i_{qs(ref)}$ according to the requested load torque through the adaptive PI controller. The field oriented control system requires the synchronous d axis current of stator coils forced to zero. Thus the peak of reference current $i_{s(ref)}$ is given by Eq. (22).

$$i_{s(ref)} = \sqrt{i_{qs(ref)}^2 + i_{ds(ref)}^2}. \qquad (22)$$

The reference current of each phase $i_{as(ref)}$, $i_{bs(ref)}$, $i_{cs(ref)}$ are function of rotor position θ_r. These reference currents are fed to the hysteresis band PWM current controller. First consider the trapezoidal current fed field oriented controlled drive. By using the value of peak reference current $i_{s(ref)}$, three phase trapezoidal reference current $i_{as(ref)}$, $i_{bs(ref)}$ and $i_{cs(ref)}$ are generated as a function of rotor position θ_r. Only the single phase trapezoidal reference current function $i_{as(ref)}(\theta_r)$ is described in Eq. (23). The $i_{bs(ref)}(\theta_r)$, $i_{cs(ref)}(\theta_r)$ similar to $i_{as(ref)}(\theta_r)$ but 120° phase displacement have to be considered.

$$i_{as(ref)}(\theta_r) = \begin{cases} i_{s(ref)} * \theta_r * \dfrac{6}{\pi}, & 0 \leq \theta_r < \dfrac{\pi}{6} \\ i_{s(ref)}, & \dfrac{\pi}{6} \leq \theta_r < \dfrac{5\pi}{6} \\ i_{s(ref)} * (\pi - \theta_r) * \dfrac{6}{\pi}, & \dfrac{5\pi}{6} \leq \theta_r < \dfrac{7\pi}{6} \\ -i_{s(ref)}, & \dfrac{7\pi}{6} \leq \theta_r < \dfrac{11\pi}{6} \\ i_{s(ref)} * (\theta_r - 2\pi) * \dfrac{6}{\pi}, & \dfrac{11\pi}{6} \leq \theta_r < 2\pi \end{cases} \quad (23)$$

Now three phase square wave reference current $i_{as(ref)}$, $i_{bs(ref)}$, $i_{cs(ref)}$ are generated corresponding to the rotor position according to the Table 1 for square current fed field oriented controlled PMBLDC motor drive. Finally three phase sinusoidal reference current $i_{as(ref)}$, $i_{bs(ref)}$, $i_{cs(ref)}$ are generated according to Eq. (24-26) as a function of rotor position.

$$i_{as(ref)} = i_{s(ref)} * \sin(\theta_r) \qquad (24)$$

$$i_{bs(ref)} = i_{s(ref)} * \sin\left(\theta_r - \frac{2\pi}{3}\right) \qquad (25)$$

$$i_{cs(ref)} = i_{s(ref)} * \sin\left(\theta_r + \frac{2\pi}{3}\right) \qquad (26)$$

Table 1. Square 3-phase reference current corresponding to rotor position

Rotor Position θ_r	$i_{as(ref)}(\theta_r)$	$i_{bs(ref)}(\theta_r)$	$i_{cs(ref)}(\theta_r)$
$0 \leq \theta_r < \dfrac{\pi}{6}$	0	$-i_{s(ref)}$	$i_{s(ref)}$
$\dfrac{\pi}{6} \leq \theta_r < \dfrac{3\pi}{6}$	$i_{s(ref)}$	$-i_{s(ref)}$	0
$\dfrac{3\pi}{6} \leq \theta_r < \dfrac{5\pi}{6}$	$i_{s(ref)}$	0	$-i_{s(ref)}$
$\dfrac{5\pi}{6} \leq \theta_r < \dfrac{7\pi}{6}$	0	$i_{s(ref)}$	$-i_{s(ref)}$
$\dfrac{7\pi}{6} \leq \theta_r < \dfrac{9\pi}{6}$	$-i_{s(ref)}$	$i_{s(ref)}$	0
$\dfrac{9\pi}{6} \leq \theta_r < \dfrac{11\pi}{6}$	$-i_{s(ref)}$	0	$i_{s(ref)}$
$\dfrac{11\pi}{6} \leq \theta_r < 2\pi$	0	$-i_{s(ref)}$	$i_{s(ref)}$

4.3. PWM Current Controller

Delta modulated current control PWM is used for the switching of voltage source inverter. In this PWM method the actual current continually tracks the reference current within hysteresis band. This hysteresis-band PWM is basically an instantaneous feedback current control technique. When the actual current exceeds upper band limit, then the upper switch has to be off and lower switch has to be on. Similarly when the actual current exceeds lower band limit, upper switch is on and lower switch is off. The switching logic which is used in these three different reference current fed control drives, is given below

If $i_{as} < (i_{as(ref)} - H_b)$
Then switch 1 is ON and switch 4 is OFF ($P_A = 1$)
If $i_{as} < (i_{as(ref)} + H_b)$
Then switch 1 is OFF and switch 4 is ON ($P_A = 0$)
If $i_{bs} < (i_{bs(ref)} - H_b)$
Then switch 3 is ON and switch is 6 OFF ($P_B = 1$)
If $i_{bs} < (i_{bs(ref)} + H_b)$
Then switch 3 is OFF and switch 6 is ON ($P_B = 0$)
If $i_{cs} < (i_{cs(ref)} - H_b)$
Then switch 5 is ON and switch 2 is OFF ($P_C = 1$)
If $i_{cs} < (i_{cs(ref)} + H_b)$
Then switch 5 is OFF and switch 2 is ON ($P_C = 0$)

Where, H_b is the hysteresis band around reference current. The inverter output voltage according to the above switching condition are given by Eq. (27-29)

$$V_{as} = \frac{1}{3}\left[2P_A - P_B - P_C\right] \quad (27)$$

$$V_{bs} = \frac{1}{3}\left[-P_A + 2P_B - P_C\right] \quad (28)$$

$$V_{cs} = \frac{1}{3}\left[-P_A - P_B + 2P_C\right]. \quad (29)$$

5. Results and Discussion

The drive system was simulated in a digital computer with a software written in C++ environment. The ratings of the simulated PMBLDC motor are described in Table 2.

Table 2. PMBLDC Motor Specifications

Specifications	Quantity
No. of Poles	8
Rated Voltage	48 V
Rated Current	2.5 Amp
Rated Speed	150 rad/s
Rated Torque	2.0 Nm
Initial Torque	0.4 Nm
Resistance/Phase	0.36 Ω
Self-Inductance	2.1 mH
Mutual inductance	1.5 mH
Flux linkages constant	0.105
Moment of Inertia	0.0048 kg-m^2
Damping constant	0.002 N-m/rad/sec
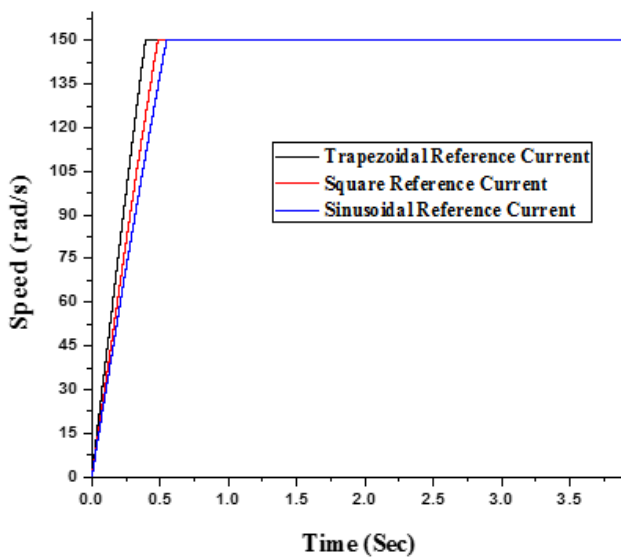
Figure 5. Starting characteristics of PMBLDC motor drives for trapezoidal, square and sinusoidal reference current fed field oriented control

5.1. Starting Characteristics

The PMBLDC motor starts with an initial load torque 0.4 Nm. Starting speed characteristics i.e. time taken by the motor to reach its rated speed (150 rad/s) with its initial torque (0.4 Nm) for trapezoidal, square and sinusoidal reference current fed field oriented controlled PMBLDC motor drives is shown in Figure 5. From Figure 5, it is seen that, PMBLDC vector controlled trapezoidal, square and sinusoidal current fed drives take 0.39, 0.48 and 0.55 seconds respectively to gain rated speed. So trapezoidal current fed field oriented control drive is suitable to gain rated speed as fast as possible. Trapezoidal reference current fed drive takes minimum time to reach its rated speed than square and sinusoidal reference current fed drives, because the torque handling capacity of trapezoidal reference current fed PMBLDC motor drive is greater than the other two reference current fed PMBLDC motor drives.

Phase currents of PMBLDC motor at the time of starting for vector controlled trapezoidal, square and sinusoidal current fed drives are depicted in Figure 6. It shows that the amplitude of 3-phase current is 2.5 Amp (rated current of the motor) at the transient time of starting for these three control drives. Started current is limited through the current limiter block as shown in Figure 4. Figure 6 also describes that after gaining rated speed i.e. at steady state motor takes maximum 0.75 Amp current for trapezoidal current fed, maximum 1.0 Amp current for square current fed and maximum 1.12 Amp current for sinusoidal current fed drives for initial torque 0.4 Nm. So that PMBLDC motor takes less current at stable condition for trapezoidal current fed drive than square and sinusoidal drives due to the capability of more load torque handling capacity.

3-phase back EMF, rotor position curve at the time of starting for vector controlled trapezoidal reference current fed PMBLDC drive is shown in Figure 7 as for example. Now the back EMF and corresponding phase current of trapezoidal, square and sinusoidal current fed field oriented control drives for steady state condition of these drives are pictured in Figure 8.

Figure 9 depicts developed electromagnetic torque in PMBLDC motor for trapezoidal, square and sinusoidal current fed field oriented controlled drives. It mainly describes the torque pulsation status for three different current fed drives. Periodic small scale torque pulsation can be seen for trapezoidal and sinusoidal current fed drives. So the average torque for both trapezoidal and sinusoidal current fed drives is nearly constant. The range of torque pulsation for sinusoidal system is smaller than trapezoidal system. Though the torque pulsation for square current fed drive is very small but there exists aperiodic torque ripple. In Figure 10, stator flux linkage trajectories i.e. flux orientation representation in the stationary αβ – axes reference frame for trapezoidal, square and sinusoidal current fed vector controlled PMBLDC motor drives are pictured.

5.2. Variable Speed Characteristics

To measure the dynamic performance for three different current fed vector controlled PMBLDC motor

drives, variable speed command is given. Motor runs at speed 100 rad/s. At 1.0 second the speed command is changed to 75 rad/s and finally at 1.5 second speed command is changed to 150 rad/s. From Figure 11, motor speed follows the reference speed sharply for trapezoidal current fed vector controlled PMBLDC motor drive than the square and sinusoidal current fed drives. For sinusoidal reference current fed drive, there is noticeable difference between reference speed and actual motor speed.

(a) For trapezoidal current fed field oriented control drive

(b) For square current fed field oriented control drive

(c) For sinusoidal current fed field oriented control drive
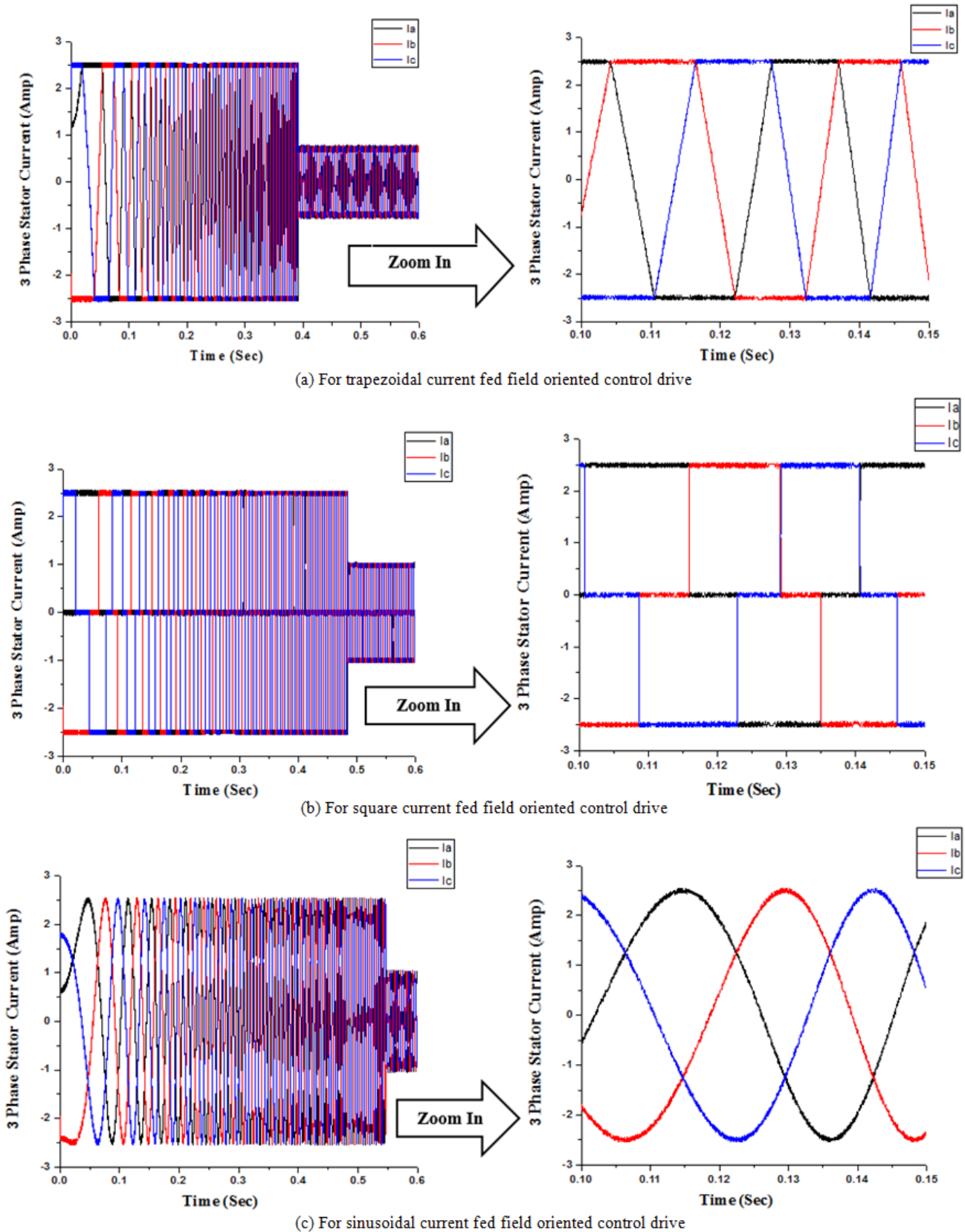
Figure 6. 3-Phase starting stator current of PMBLDC motor for trapezoidal, square and sinusoidal current fed field oriented control drive
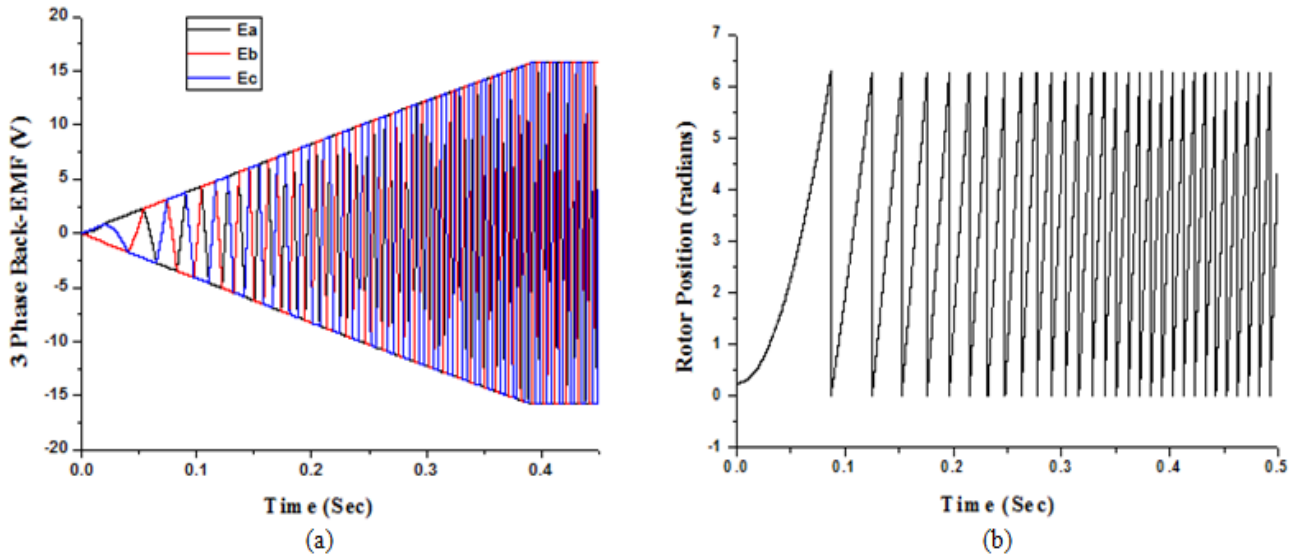
Figure 7. (a) 3-phase back EMF at starting and (b) rotor position of trapezoidal current fed field oriented controlled PMBLDC motor drive
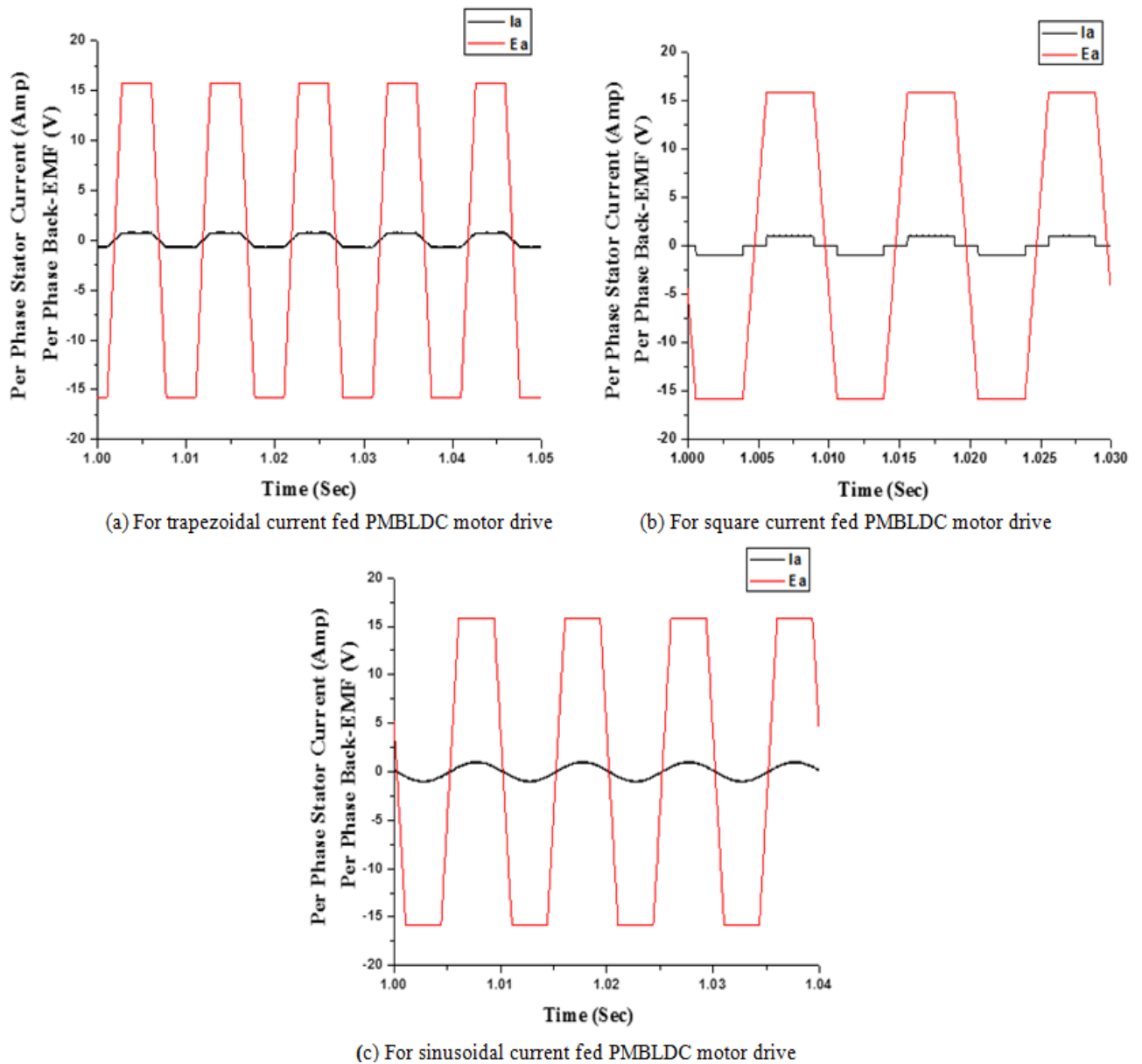
Figure 8. Per phase back EMF and corresponding phase current for Trapezoidal, Square and Sinusoidal current fed field oriented control drives
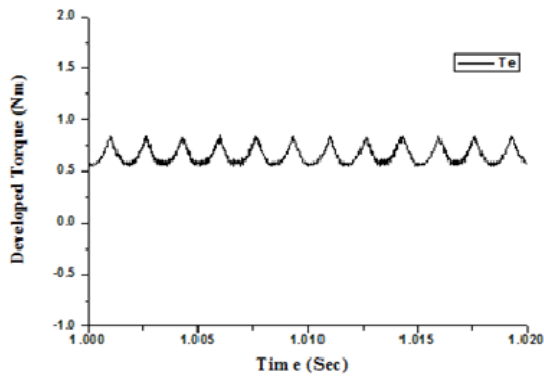
(a) Developed electromagnetic torque of trapezoidal current fed field oriented control drive
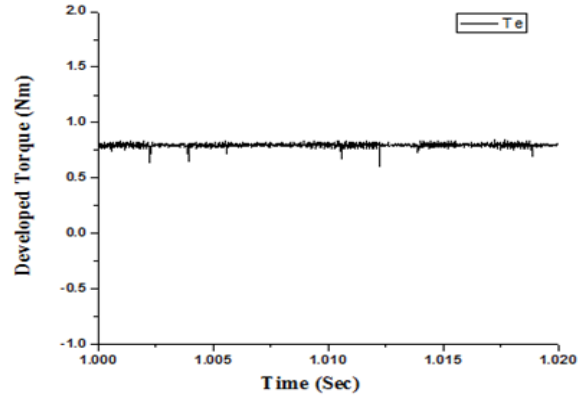
(b) Developed electromagnetic torque of square current fed field oriented control drive
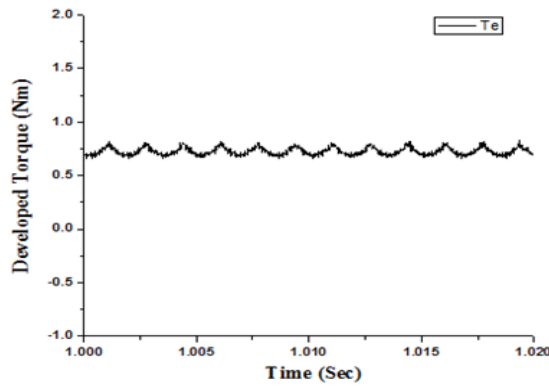
(c) Developed electromagnetic torque of sinusoidal current fed field oriented control drive

Figure 9. Torque developed for Trapezoidal, Square and Sinusoidal current fed field oriented controlled drives
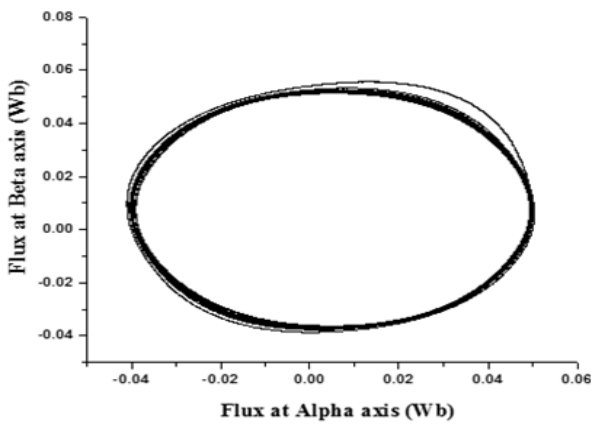
(a) For trapezoidal current fed field oriented control
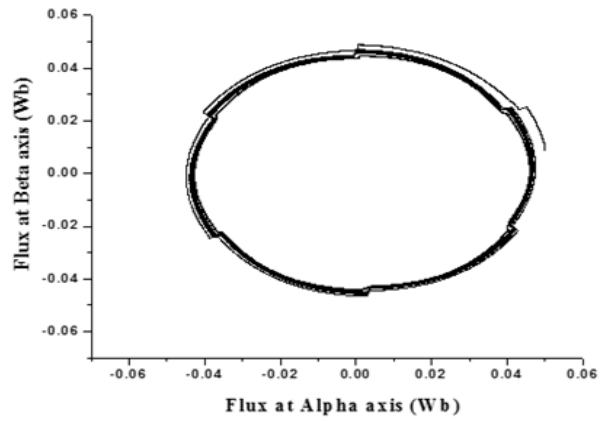
(b) For square current fed field oriented control
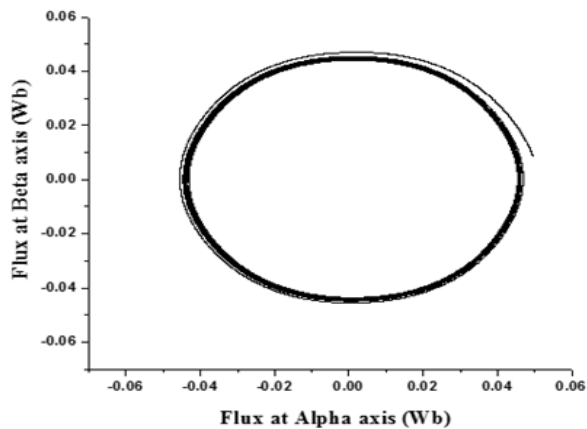
(c) For sinusoidal current fed field oriented control

Figure 10. Flux linkage trajectories in the stationary αβ axes reference frame for trapezoidal, square and sinusoidal current fed vector controlled PMBLDC motor drives
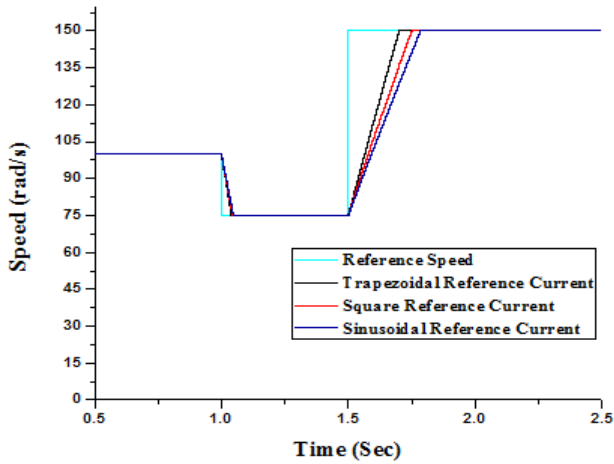
Figure 11. Comparison between speed responses of PMBLDC motor for trapezoidal, square and sinusoidal current fed vector controlled drives at dynamic speed changing condition

From 3-phase current curve for variable speed condition for three different current fed system as shown in Figure 12, it is seen that, at 1.0 second when the reference speed changes from 100 rad/s to 75 rad/s, there exists no high value of transient current beyond the limit of rated current (2.5 Amp) and no undershoot from reference speed for these three different current fed drives. Besides there is no overshoot at 1.5 second, when the reference speed goes to 150 rad/s from 75 rad/s. Condition of back EMF at the time of variable speed for trapezoidal current fed drive is shown in Figure 13.

5.3. Performance due to Load Torque Change

Now performance of PMBLDC motor vector controlled drives are determined under the condition of load torque change. At first motor runs at 150 rad/s rated speed with initial load torque 0.4 Nm. At time 1.0 second motor is loaded with its rated load torque 2.0 Nm. At that condition only trapezoidal current fed drive can sustain motor speed to its rated value 150 rad/s. But square and sinusoidal current fed drives cannot sustain its previous speed as shown in Figure 14. The speed of square and sinusoidal current fed vector controlled drives are gradually decreased after the loading of the motor. It verifies that the load torque handling capacity of square and sinusoidal current fed vector controlled PMBLDC motor drives is very poor than trapezoidal current fed vector controlled drive.
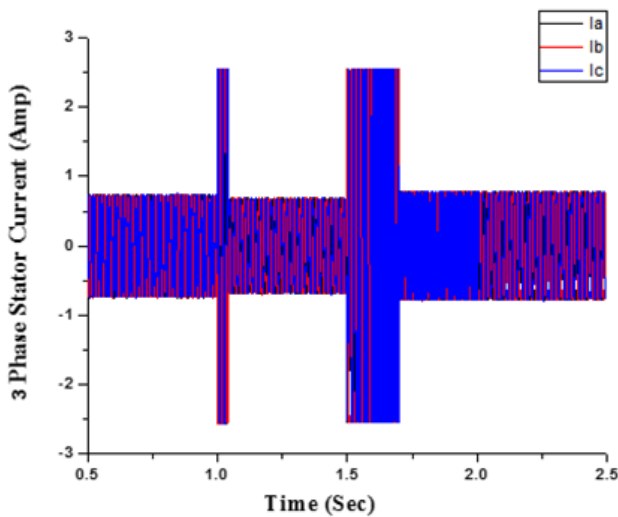
(a) For trapezoidal current fed field oriented control
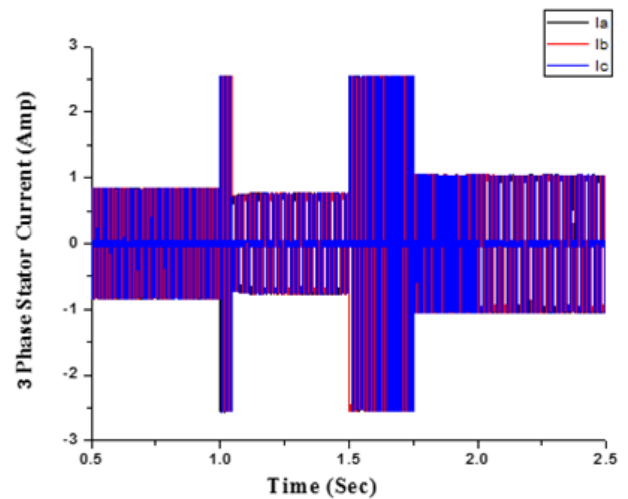
(b) For square wave current fed field oriented control
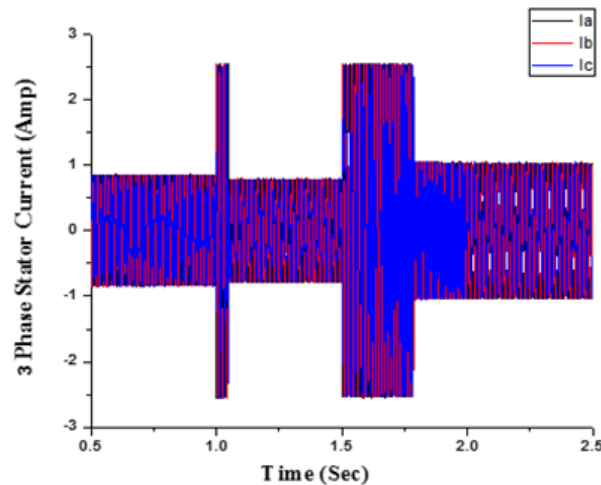
(c) For sinusoidal current fed field oriented control

Figure 12. 3-phase current of PMBLDC motor for trapezoidal, square and sinusoidal current fed field oriented controlled drive for variable speed condition considering transient current at the interface of speed changes
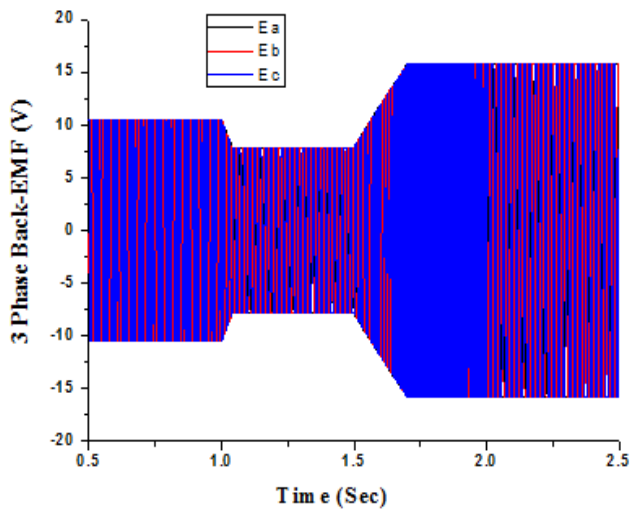
Figure 13. 3-phase back EMF at dynamic speed changing condition for trapezoidal current fed vector controlled PMBLDC motor drive
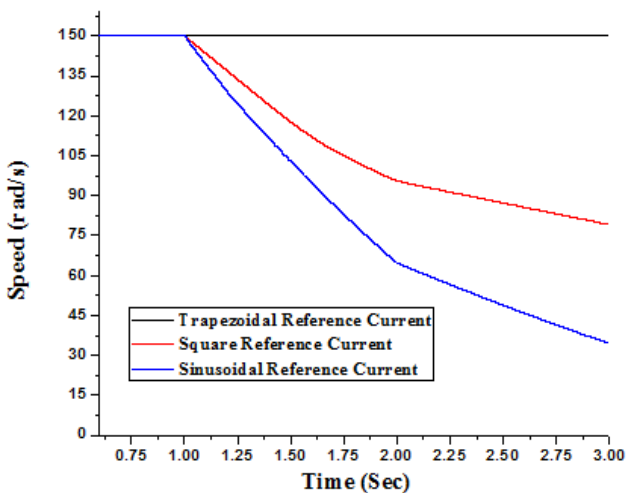
Figure 14. Speed characteristics of PMBLDC motor for sudden load torque change at 1.0 second from initial load torque 0.4 Nm to rated load torque 2.0 Nm for trapezoidal, square and sinusoidal current fed field oriented control drives

In Figure 14, the rate of gradually fall down of speed of sinusoidal current fed drive (To limit current in rated value 2.5 Amp) is higher than the rate of square wave current fed drive. Maximum load torque have to be given to the vector controlled PMBLDC motor without hampering the drive stability for square and sinusoidal current fed drives are 1.60 Nm and 1.55 Nm respectively. I.e. when square current fed drive is used to control the specified (From Table 2) PMBLDC motor, the maximum torque generating capacity is 1.60 Nm. For sinusoidal current drive, it is 1.55 Nm. Beyond these torque limit the motor cannot sustain its steady state characteristics. Thus only by using trapezoidal current fed drive, the maximum load torque handling capacity of that specified motor can be increased 25% than the square current fed drive and can be increased 29.03% than sinusoidal current fed drive.

From graphical representation of 3-phase stator current for sudden load torque change of trapezoidal current fed drive as shown in Figure 15, it summaries that, at stable reference speed stator current decreases to 0.75 Amp. But when the rated load torque is applied, the stator current is about its rated value (2.5 Amp).
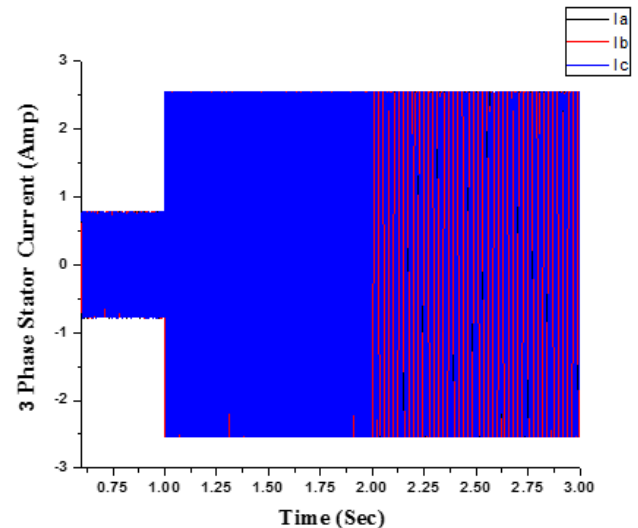
Figure 15. 3-phase stator current of trapezoidal current fed field oriented controlled PMBLDC motor drives for sudden load torque change at 1.0 second

6. Conclusion

An adaptive PI speed controller based vector controlled three different trapezoidal, square and sinusoidal reference current fed delta modulated PMBLDC motor drives are designed in this paper. This paper mainly presents how to increase the load torque handling capacity of vector controlled PMBLDC motor drives only by changing the reference current of a current fed delta modulated inverter. Individually trapezoidal, square and sinusoidal reference current fed vector controlled PMBLDC motor drives are implemented and compared among them. It is seen from the results that, only by using trapezoidal reference current fed drive instead of sinusoidal current fed drive, the load torque handling capacity can be increased form 1.55 Nm to 2.0 Nm (Rated torque of the machine). Load torque handling capacity of square current fed PMBLDC motor drive (1.60 Nm) is higher than the sinusoidal current fed drive (1.55 Nm). By considering starting, dynamic speed and load torque changing characteristics, it is clear that, the performance of trapezoidal current fed vector controlled drive is superior to the square and sinusoidal vector controlled drives. Though torque pulsation is to be considered, which is in acceptable limit. Both the starting and dynamic characteristics of trapezoidal current fed vector controlled PMBLDC motor drive is outstanding. But this performance is not superior than vector controlled voltage fed PMBLDC motor drives. It is the limitation of this paper.

References

[1]   Mourad Masmoudi, Bassem El Badsi and Ahmed Masmoudi, "Direct Torque Control of Brushless DC Motor Drives with Improved Reliability," *IEEE Transaction on Industry Applications*, 5 (6), 3744-3753, Nov.-Dec. 2014.

[2]   Salih Baris Ozturk, William C. Alexander and Hamid A.Toliyat, "Direct Torque Control of Four-Switch Brushless DC Motor with Non-Sinusoidal Back EMF," *IEEE Transaction on Power Electronics*, 25 (2), 263-271, Feb. 2010.

[3] Changliang Xia, Guokai Jiang, Wei Chen and Tingna Shi, "Switching-Gain Adaptation Current Control for Brushless DC Motors," *IEEE Transaction on Industrial Electronics* 63, 2044-2052, Apr. 2016.

[4] H. K. Samitha Ransara and Udaya K. Madawala, "A Torque Ripple Compensation Technique for a Low Cost Brushless DC Motor Drive," *IEEE Transaction on Industrial Electronics* 62 (10), 6171-6182, Oct. 2015.

[5] Yong Liu, Z. Q. Zhu and D. Howe, "Direct Torque Control of Brushless DC Drives with Reduced Torque Ripple," IEEE Transactions on Industry Applications 41 (2), 599-608, March-Apr. 2005.

[6] Protik Chandra Biswas, Bashudeb Chandra Ghosh and Md. Ashraful Islam, "Field Oriented Control of a Current Fed PMBLDC Motor and Its Comparison to Scalar Control Drive," *AIUB Journal of Science and Engineering*, 15 (1), 15-24, Aug. 2016.

[7] M.V. Ramesh, J. Amarnath, S. Kamakshaiah and G. S. Rao, "Speed Control of Brushless DC Motor by using Fuzzy Logic PI Controller," *ARPN Journal of Engineering and Applied Sciences* 6 (9), 55-62, Sep. 2011.

[8] Sung Jun Park, Han Woong Park, Man Hyung Lee and Fumio Harashima, "A New Approach for Minimum-Torque-Ripple Maximum-Efficiency Control of BLDC Motor," *IEEE Transaction on Industrial Electronics* 47 (1), 109-114, Feb. 2000.

[9] Junhwi Park, Yunchang Kwak, Yeongjun Jo, Jongnam Bae and Dong-Hee Lee, "Torque Ripple Reduction of BLDC motor using Predicted Current Control," *IEEE Transportation Electrification Conference and Expo*, Asia- Pacific (ITEC), Busan, Korea, 407-411, Jun. 2016.

[10] Marek Lazor and Marek Stulrajter, "Modified Field Oriented Control for Smooth Torque Operation of a BLDC Motor," *Technically IEEE sponsored ELEKTRO conference*, Rajecke Teplice, 180-185, May 2014.

[11] Virginia Manzolini, Araz Darba and Frederik De Belie, "Improving the Torque Generation in Self-Sensing BLDC Drives by Shaping the Current Waveform," *2016 International Symposium on Power Electronics, Electrical Drives, Automation and Motion*, 510-515, Jun. 2016.

[12] Chenjun Cui, Gang Liu and Kun Wang, "A Novel Drive Method for High-Speed Brushless DC Motor Operating in a Wide Range," *IEEE Transaction on Power Electronics,* 30 (9), 4998-5008, Sep. 2015.

[13] Anders Kronberg, "Design and Simulation of Field Oriented Control and Direct Torque Control for a Permanent Magnet Synchronous Motor with Positive Saliency," *Uppsala Universitet*, 12-20, 2012.

[14] "Optimum Vector Control for Brushless Motors," *Toshiba* Available: http://www.newelectronics.co.uk/articleimages/25930%5CMotor %20Control%20Solutions.pdf. [Accessed Oct. 10, 2016].